

# Chelidonine enhances the antitumor effect of lenvatinib on hepatocellular carcinoma cells

This article was published in the following Dove Press journal:  
*OncoTargets and Therapy*

Fang-jie Hou  
Li-xiao Guo  
Kai-yan Zheng  
Jun-na Song  
Qian Wang  
Yu-guang Zheng

Hebei University of Chinese Medicine,  
Shijiazhuang City, Hebei Province 050200,  
People's Republic of China

**Background:** Lenvatinib is a newly approved molecular targeted drug for the treatment of advanced hepatocellular carcinoma (HCC). However, the high cost associated with this treatment poses a huge financial burden on patients and the entire public health system. Therefore, there is an urgent need to develop novel strategies that enhance the antitumor effect of lenvatinib.

**Methods:** The antitumor effects of chelidonine or/and lenvatinib on HCC cell lines MHCC97-H and LM-3 were examined using the 3-[4,5-dimethyl-2-thiazolyl]-2,5-diphenyl-2-H-tetrazolium bromide (MTT) assay. For the in-vivo investigation, the effect on subcutaneous or intrahepatic tumor growth in nude mice was also determined. The mRNA levels of epithelial mesenchymal transition (EMT)-related factors were examined through quantitative polymerase chain reaction or Western blot.

**Results:** In the present study, we found that treatment with chelidonine enhanced the apoptotic effect of lenvatinib on HCC cells and the in-vivo growth of HCC tumors in nude mice. Mechanistically, treatment with chelidonine increased the expression of epithelial indicator E-cadherin, whereas it decreased the expression of mesenchymal indicators N-cadherin and Vimentin. These findings suggest that chelidonine restricted the EMT in HCC cells.

**Conclusion:** Chelidonine inhibits the process of EMT and enhances the antitumor effect of lenvatinib on HCC cells.

**Keywords:** advanced hepatocellular carcinoma, lenvatinib, chelidonine, epithelial mesenchymal transition

## Introduction

In China, there are >70 million patients with liver disease who suffer from various chronic liver diseases caused by hepatitis B virus infection.<sup>1</sup> Unfortunately, a large proportion of these patients eventually progresses into hepatocellular carcinoma (HCC).<sup>2,3</sup> HCC seriously endangers the longevity of humans, and poses a huge challenge to the public health system.<sup>4</sup> Moreover, most patients suffering from HCC are initially diagnosed an advanced stage, and only a very small proportion are suitable to receive radical treatments, such as surgical resection.<sup>5,6</sup> Molecular targeted chemotherapy, represented by orally administrable kinase inhibitors (eg, sorafenib), is the top therapeutic choice for the treatment of advanced HCC.<sup>7,8</sup> Small molecular inhibitors of receptor protein tyrosine kinases, such as vascular endothelial growth factor receptor (VEGFR) and mitogen-activated protein kinase, can inhibit the proliferation and metastasis of HCC cells and tumor angiogenesis.<sup>9</sup> However, the application of HCC molecular targeted drugs is faced with several

Correspondence: Kai-yan Zheng  
Hebei University of Chinese Medicine,  
No. 3 Xingyuan Road, Luquan Economic  
Development Zone, Shijiazhuang City,  
Hebei Province 050200, People's Republic  
of China  
Tel +86 311 8992 6017  
Fax +86 311 8992 6017  
Email zhengkaiyan168@126.com

challenges. Firstly, only 26–43% of patients with advanced HCC are sensitive to sorafenib.<sup>10</sup> Secondly, those who are sensitive to sorafenib are likely to become tolerant to the drug as the treatment progresses.<sup>10</sup> In addition, other drugs (ie, regorafenib and lenvatinib), which have been applied in the clinic for a short period of time, may be linked to the development of resistant if widely used. Thirdly, the currently available molecular targeted therapies for advanced HCC are very expensive, thereby imposing a significant financial burden. Fourthly, at present, the dosage of the oral administration of such kinase inhibitors is relatively high (eg, sorafenib: 800 mg/day). This high dosage may induce several side effects, such as gastrointestinal bleeding.<sup>11,12</sup> The presence of advanced HCC is often accompanied by varying degrees of cirrhosis, which renders the long-term, high-dose, oral administration of molecular targeted drugs inducing some problems in terms of safety.<sup>13,14</sup> Therefore, it is important to develop therapeutic strategies to achieve the safer and more effective treatment for each agent.

Chelidonine is a natural product extracted from *Chelidonium majus* L.<sup>15,16</sup> Previously, chelidonine was widely used for anesthetic purposes.<sup>17,18</sup> Recently, chelidonine has also been shown to possess antitumor activity.<sup>19,20</sup> It is well known that natural products have been widely used and considered as an auxiliary medication to enhance the sensitivity of antitumor agents.<sup>21–24</sup> In the present study, the antitumor effect of chelidonine was examined in HCC cells.

## Materials and methods

### Agents and cell culture

L-02 (a non-tumor hepatic cell line) or HCC cell lines (MHCC97-H and LM-3) were donated by Dr. Fan Feng at the Department of Pharmacy, General Hospital of Shenyang Military Area Command (Shenyang, China).<sup>25,26</sup> H22 (Cat. No. BNCC338327), a mouse HCC cell line, was purchased from BeNa Culture Collection Corporation (Beijing, China). All cells were purchased from the culture collection centers of the Chinese government, namely the Type Culture Collection of the Chinese Academy of Sciences (Shanghai, China) and the National Infrastructure of Cell Line Resources, Chinese Academy of Medical Sciences (Beijing, China). Lenvatinib (Cat. No. S1164) and chelidonine (Cat. No. S9154) were purchased from Selleck Corporation, (Houston, TX, USA). Dimethyl sulfoxide (DMSO) was purchased from Sigma Aldrich

Corporation (St. Louis, MO, USA). The usage of cell lines was approved by the Ethics Committee of Hebei University of Chinese Medicine (Shijiazhuang City, Hebei Province, China). HCC cells were cultured in Dulbecco's Modified Eagle's Medium (DMEM; Thermo Scientific Corporation, Waltham, MA, USA) supplemented with fetal bovine serum (FBS; Thermo Scientific Corporation).

### Examination of cell survival

Lenvatinib or chelidonine was firstly dissolved in DMSO, and DMEM was subsequently added to the solution. The hepatic cells, which were cultured in DMEM with 10% FBS at 37 °C with 5% CO<sub>2</sub> condition, were seeded into 96-well plates (Corning Corporation, Corning, NY, USA) with 8,000 cells/well, and treated with the indicated concentration of lenvatinib or chelidonine (Table 1) for 48 h. Subsequently, the cells were examined using the 3-[4,5-dimethyl-2-thiazolyl]-2,5-diphenyl-2-H-tetrazolium bromide (MTT) assay. The MTT were treated the cells for 4–6 hrs and the cells were lysis by using DMSO. The optical density (OD) values of cell samples were examined at 490 nm. Following the MTT experiments, the inhibition rates on the survival of HCC cells and the half maximal inhibitory concentration (IC<sub>50</sub>) of the agents were calculated as described by Feng et al (2013).<sup>27</sup> The inhibition on HCC cells were calculated as follows: [(OD values of control group cells examined at 490 nm control group cells) – (OD values of administration group cells examined at 490 nm control group cells)]/(OD values of control group cells examined at 490 nm control group cells) × 100%.<sup>28,29</sup> The IC<sub>50</sub> of the agents were calculated based on the inhibition rates, to reflect their antitumor effect on HCC cells.

### Quantitative polymerase chain reaction (qPCR)

HCC cells were treated with the indicated concentrations of agents (Table 1). Subsequently, the cells were harvested and the total RNA was extracted using a PARIS™ Kit (Thermo Scientific Corporation). The RNA samples were reverse transcribed using a Multiscribe™ Reverse Transcriptase (Thermo Scientific Corporation). The qPCR experiments were performed as described by Ji et al (2017) and Liang et al (2017).<sup>30,31</sup> GAPDH (glyceraldehyde-3-phosphate dehydrogenase) was selected as the loading control. The relative mRNA expression levels of E-cadherin, N-cadherin, Vimentin, Twist, and Snail were

**Table 1** The concentrations of Chelidonine or Lenvatinib used in cell survival examination

Agents	Concentration ( $\mu\text{mol/L}$ )						
	0.03	0.1	0.3	1	3	10	30
Chelidonine	0.03	0.1	0.3	1	3	10	30
Lenvatinib	0.003	0.01	0.03	0.1	0.3	1	3

**Table 2** Primers used in qPCR experiments

Genes	Primers	Sequences
N-cadherin	Forward Sequence	CCTCCAGAGTTTACTGCCATGAC
	Reverse Sequence	GTAGGATCTCCGCCACTGATTC
Vimentin	Forward Sequence	AGGCAAAGCAGGAGTCCACTGA
	Reverse Sequence	ATCTGGCGTTCCAGGGACTCAT
Snail	Forward Sequence	TGCCCTCAAGATGCACATCCGA
	Reverse Sequence	GGGACAGGAGAAGGGCTTCTC
Twist	Forward Sequence	GCCAGGTACATCGACTTCCTCT
	Reverse Sequence	TCCATCCTCCAGACCGAGAAGG
E-cadherin	Forward Sequence	AAGGCACGCCTGTCTGAAGCA
	Reverse Sequence	ACGTTGTCCCGGTGTCATCCT

calculated using the comparative  $C_T$  method.<sup>30,31</sup> The primers used in this experiment are shown in [Table 2](#).

## Antibodies and Western blotting

HCC cells were firstly treated with the indicated concentrations of chelidonine ([Table 1](#)). Western blotting was performed using a standard protocol. Briefly, cells were harvested and the total protein of cells was extracted. Subsequently, the protein samples were subjected to sodium dodecyl sulfate polyacrylamide gel electrophoresis (SDS-PAGE). After SDS-PAGE, the protein in the SDS-PAGE gel were transferred onto a polyvinylidene fluoride membrane. Subsequently, the membrane was blocked using 5% bovine serum albumin diluted in Tris-buffered saline with Tween (TBST) buffer. After blocking, the membrane was incubated with primary antibodies diluted by TBST. After three washes with TBST, the membrane was incubated with secondary antibodies. The membrane was visualized using an enhanced chemiluminescence kit (Amersham Biosciences, Piscataway, NJ, USA). Western blotting was performed using antibodies purchased from Abcam Corporation (Cambridge, UK) against E-cadherin (Cat. No. ab15148; dilution rate: 1:500), N-cadherin (Cat. No. ab98952; dilution rate: 1:1000), Vimentin (Cat. No. ab8069; dilution rate: 1:2000), Twist (Cat. No. ab49254; dilution rate:

1:500), Snail (Cat. No. ab216347; dilution rate: 1:500), or GAPDH (Cat. No. ab8245; dilution rate: 1:5000).

## Assessment of subcutaneous tumor growth

The animal experiments performed in this study were approved by the Ethics Committee of Animal Care and Usage, of the Hebei University of Chinese Medicine. All animal experiments were performed in accordance with the UK Animals (Scientific Procedures) Act, 1986 and associated guidelines. The nude mice or BalB/c mice used in this study were purchased from Sibeifu Corporation (Beijing, China). HCC cells were cultured and harvested to prepare the cell suspension, which was diluted using physiological saline. Subsequently, cell suspensions ( $5 \times 10^6$  cells/animal) were injected into subcutaneous position (sites) of nude mice.<sup>32,33</sup> The mice received oral administration of agents 4–5 days following the injection of HCC cells. For the chelidonine alone treatment, the mice received the indicated concentrations of chelidonine ([Table 3](#)). For the lenvatinib–chelidonine combination treatment, the mice received solvent control (physiological saline) plus the indicated concentration of lenvatinib ([Table 3](#)) or 5 mg/kg chelidonine plus the indicated concentration of lenvatinib ([Table 3](#)). The mice received the agents orally once every 2 days. Following the administration of 10 doses over a 21-day period, the tumors were harvested and their volumes and weights were examined as described by Jia et al (2016)

**Table 3** The concentrations of Chelidonine or Lenvatinib used in animal examination

Agents	Concentration (mg/kg)					
	1	2	5	10	20	30
Chelidonine	1	2	5	10	20	30
Lenvatinib	0.05	0.1	0.2	0.5	1	2

and Xie et al (2018).<sup>24,34</sup> Tumor volumes were calculated as follows: (tumor length) × (tumor width) × (tumor width)/2. The inhibition rates induced by agents on the subcutaneous growth of HCC cells were calculated as follows: (Control group's tumor volume – administration group's tumor volume)/(Control group's tumor volume) × 100% or (Control group's tumor weights – administration group's tumor weights)/(Control group's tumor weights) × 100%.

Moreover, mice possessing a normal immune system, ie, BALB/c mice (Sibeifu Corporation, Beijing, China), were used. H22 cells were injected into BALB/c mice to form subcutaneous tumors. The mice received oral administration of agents 4–5 days following the injection of HCC cells. For chelidonine alone treatment, the mice received the indicated concentrations of chelidonine (Table 3). For the lenvatinib–chelidonine combination treatment, the mice received solvent control (physiological saline) plus the indicated concentration of lenvatinib (Table 3) or 5 mg/kg chelidonine plus the indicated concentration of lenvatinib (Table 3). The mice received the agents orally once every 2 days. Following the administration of 10 doses over a 21-day period, the tumors were harvested and their volumes and weights were examined as described by Jia et al (2016) and Xie et al (2017).<sup>24,34</sup> Tumor volumes were calculated as follows: (tumor length) × (tumor width) × (tumor width)/2. The inhibition rates induced by the agents on the subcutaneous growth of HCC cells were calculated as follows: (Control group's

tumor volume – administration group's tumor volume)/(Control group's tumor volume) × 100% or (Control group's tumor weights – administration group's tumor weights)/(Control group's tumor weights) × 100%.

### Intrahepatic growth experiments

MHCC97-H cells) were firstly seeded into nude mice to form subcutaneous tumor tissues. Following the formation of subcutaneous tumors in nude mice, the tumor tissues were harvested, and micro-blocks of tumor tissues were prepared (Table 4). Subsequently, the micro-blocks were injected into the liver of nude mice.<sup>35–38</sup> The mice received oral administration of agents 4–5 days after injection of the tumor tissue micro-blocks. Subsequently, the animals were divided into four groups: (1) solvent control group; (2) 5 mg/kg chelidonine treatment group; (3) 0.5 mg/kg lenvatinib treatment group; and (4) 5 mg/kg chelidonine plus 0.5 mg/kg lenvatinib treatment group. For each group, the mice received the agents orally once every 2 days. Following the administration of 10 doses over a 21-day period, the livers of mice with tumor tissues (ie, lesions/nodules) were harvested and collected. The photographs of livers were quantitatively analyzed using the Image J software (National Institutes of Health, Bethesda, MD, USA) as described by Xie et al (2018) and Chen et al (2018).<sup>34,39</sup> The intrahepatic growth of MHCC97-H cells was measured by calculating the relative lesion/nodule area as follows:

**Table 4** Weight of Tumor tissues seeded into nude mice's liver organ

Tumor tissues	Weight of Tumor tissues (mg)			
	Solvent control	Chelidonine	Lenvatinib	Chelidonine + Lenvatinib
No. 1	2.08	1.92	2.05	2.10
No. 2	2.06	1.8	2.14	1.96
No. 3	2.11	2.13	1.95	2.03
No. 4	2.19	1.98	2.22	2.12
No. 5	1.98	1.83	1.75	1.84
No. 6	1.79	1.71	1.75	1.96
No. 7	1.74	1.99	1.91	2.09
No. 8	2.06	2.03	2.02	1.77
No. 9	1.99	1.78	1.85	2.01
No. 10	1.76	2.25	1.99	2.03

(total intensity of lesion)/(total intensity of liver organ)  $\times 100\%$ . The inhibition rates of agents on the intrahepatic growth of MHCC97-H cells were calculated as follows: [(control group relative lesion/nodule area) - (administration group relative lesion/nodule area)]/(control group relative lesion/nodule area)  $\times 100\%$ .<sup>34,39</sup>

## Statistical analysis

Statistical analyses were performed via two-way analysis of variance with Bonferroni correction, using the SPSS software (Version No.: 9.0; IBM Corporation, Armonk, NY, USA). *P*-values  $< 0.05$  denoted statistical significance. The  $IC_{50}$  values were calculated using the Origin software (Northampton, MA, USA).

## Results

### Chelidonine enhances the sensitivity of HCC cells to lenvatinib

Firstly, the antitumor effect of chelidonine on HCC cells was examined. As shown in Figure 1A and B, chelidonine inhibits the survival of MHCC97-H cells (Figure 1A) and LM-3 (Figure 1B) in a dose-dependent manner. The  $IC_{50}$  values of chelidonine in MHCC97-H and LM3 cells were  $7.72 \pm 0.70 \mu\text{mol/L}$  and  $6.34 \pm 0.44 \mu\text{mol/L}$ , respectively.

Epithelial mesenchymal transition (EMT) is a critical process for tumor cell survival. Therefore, we subsequently tested the effect of chelidonine on EMT. As shown in Figure 2, chelidonine reduced the expression of mesenchymal markers N-cadherin and Vimentin, whereas it enhanced the expression of the epithelial marker E-cadherin (Figure 2). These results suggested that chelidonine induced EMT in HCC cells. In addition, treatment with chelidonine inhibited the expression of Twist and Snail, the two key regulators of the EMT process (Figure 2). Chelidonine significantly inhibited the viability of HCC cells at the concentrations of 3, 10, and  $30 \mu\text{mol/L}$ . Notably, chelidonine at the  $1 \mu\text{mol/L}$  concentration did not exert a significant injury on cell viability. Nevertheless,  $1 \mu\text{mol/L}$  of chelidonine inhibited the EMT process in HCC cells. Therefore,  $1 \mu\text{mol/L}$  is a non-cytotoxic dose of chelidonine that can affect the EMT process of HCC cells. Thus, this concentration was selected for the following studies. Subsequently, the effect of the combination of chelidonine and lenvatinib on HCC cells was examined. As shown in Figure 1C and D, treatment with chelidonine enhanced the antitumor effect of lenvatinib on HCC cells ( $IC_{50}$  values are shown in Table 5).

L-02 cells were also used to further examine the effect of chelidonine or lenvatinib. The inhibitory effect of

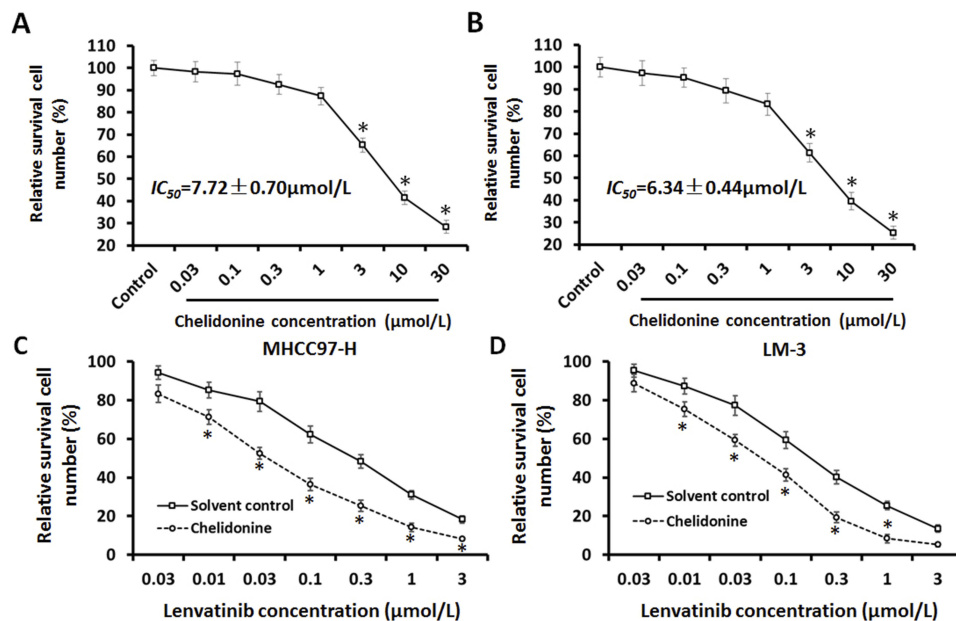


**Figure 1** The antitumor effect of chelidonine on HCC cells. HCC cells, MHCC97-H (A), and LM-3 (B) were treated with the indicated concentration of chelidonine for 48 h. Subsequently, the cells were harvested for analysis using the MTT assay. The results are shown as the mean  $\pm$  SD of the inhibition rate induced by chelidonine on the survival of HCC cells. HCC cells, MHCC97-H (C), and LM-3 (D), which were pre-treated with  $1 \mu\text{mol/L}$  chelidonine, were treated with the indicated concentration of lenvatinib for 48 h. Subsequently, the cells were harvested for analysis using the MTT assay. The results are shown as the mean  $\pm$  SD from the inhibition rate induced by chelidonine on the survival of HCC cells.

**Notes:** \* $P < 0.05$  versus solvent control with chelidonine.

**Abbreviations:** HCC, hepatocellular carcinoma; MTT, 3-(4,5-dimethyl-2-thiazolyl)-2,5-diphenyl-2-H-tetrazolium bromide; SD, standard deviation.



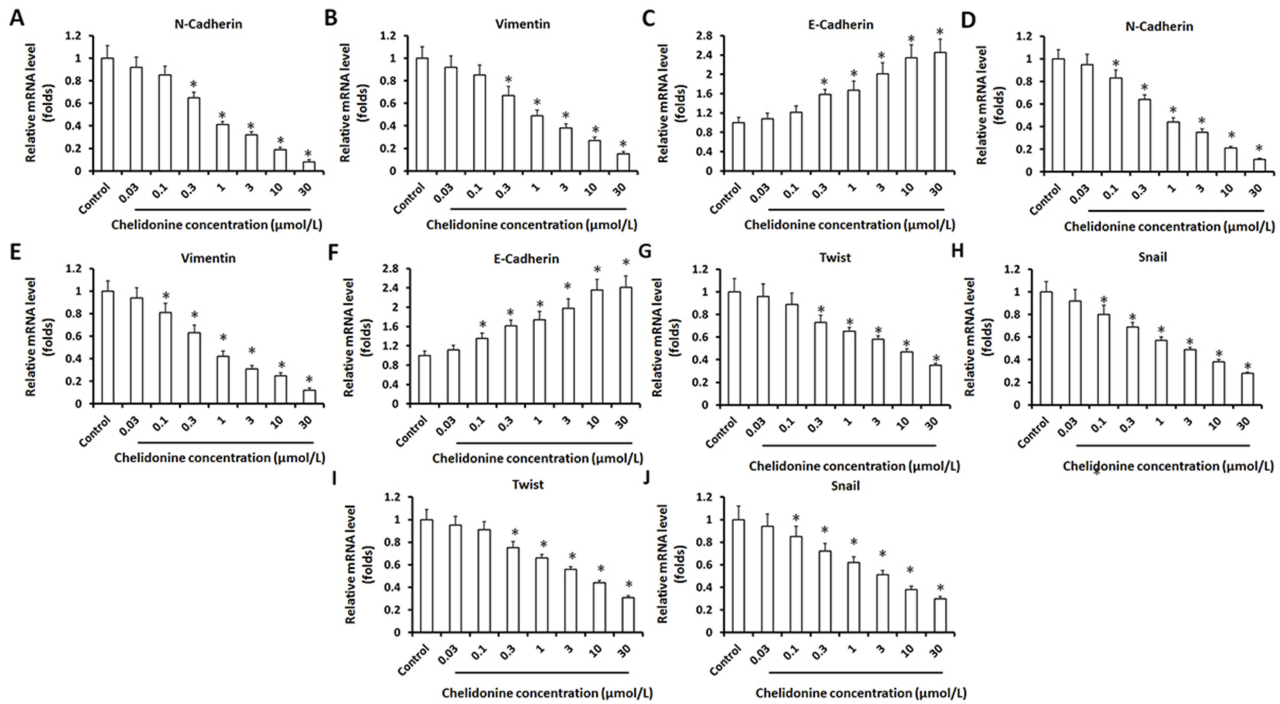


**Figure 2** The effect of chelidonine on EMT indicators in cultured HCC cells or HCC cells in subcutaneous tumor tissues. HCC cells, MHCC97-H (A–C), and LM-3 (D–F) were treated with the indicated concentration of chelidonine for 48 h. Subsequently, the cells were harvested and the total RNA was extracted from cells. The expression of N-cadherin (A and D), Vimentin (B and E), and E-cadherin (C and F) was examined through qPCR. The results are shown as the mean±SD from the qPCR experiments. HCC cells, MHCC97-H (G and H), and LM-3 (I and J) were treated with the indicated concentration of chelidonine for 48 h. Subsequently, the cells were harvested and the total RNA was extracted from cells. The expression of Twist (G and I) and Snail (H and J) was examined through qPCR. The results are shown as the mean ± SD from the qPCR experiments.

**Notes:** \**P*<0.05 versus solvent control with chelidonine.

**Abbreviations:** EMT, epithelial-mesenchymal transition; HCC, hepatocellular carcinoma; qPCR, quantitative polymerase chain reaction; SD, standard deviation.

**Table 5** The IC<sub>50</sub> values of Lenvatinib on HCC cells

Cell lines	Solvent control	Chelidonine
	IC <sub>50</sub> value of Lenvatinib (nmol/L)	
MHCC97-H	260.02±14.4	42.86±2.43
LM-3	185.26±6.36	52.28±3.12

lenvatinib on L-02 cells was much lower than that observed in HCC cells; the IC<sub>50</sub> value of lenvatinib in L-02 cells was 8.53±0.55 μmol/L. Treatment with chelidonine enhanced the effect of lenvatinib on L-02 cells, and the IC<sub>50</sub> values of lenvatinib decreased from 8.53±0.55 μmol/L to 2.67±0.33 μmol/L. Therefore, chelidonine may enhance the sensitivity of HCC cells to lenvatinib.

### Chelidonine increases the in-vivo antitumor activity of lenvatinib against HCC tumors

A subcutaneous tumor model in nude mice was established to further examine the synergistic effect of lenvatinib. As shown in Figure 3, chelidonine inhibited the subcutaneous growth of MHCC97-H cells in a dose-dependent manner.

Chelidonine decreased the mRNA or protein levels of N-cadherin, Vimentin, Twist, and Snail, whereas it enhanced the expression of E-cadherin (Figures 4 and 5). As expected, the non-cytotoxic concentration (5 mg/kg) of chelidonine inhibited the EMT process of HCC cells in subcutaneous tumors. As shown in Figure 6, at non-cytotoxic concentrations, the combination of chelidonine with lenvatinib enhanced the antitumor effect of lenvatinib. The IC<sub>50</sub> values of lenvatinib in the subcutaneous growth of MHCC97-H cells decreased from 0.82±0.05 mg/kg to 0.18±0.02 mg/kg. Moreover, the effect of chelidonine or lenvatinib on H22 cells, a liver cancer cell line of mice, in normal mice (BalB/c) was also examined (Figure S1). The inhibitory effect of lenvatinib on the subcutaneous growth of H22 cells was much lower than that observed in HCC cells. In addition, treatment with chelidonine at a concentration with no significant toxicity enhanced the antitumor effect of lenvatinib on the subcutaneous growth of H22 cells.

Subsequently, we performed an analysis of the combination treatment in the intrahepatic tumor model. As shown

OncoTargets and Therapy downloaded from https://www.dovepress.com/ by 146.185.203.32 on 19-Aug-2019 For personal use only.

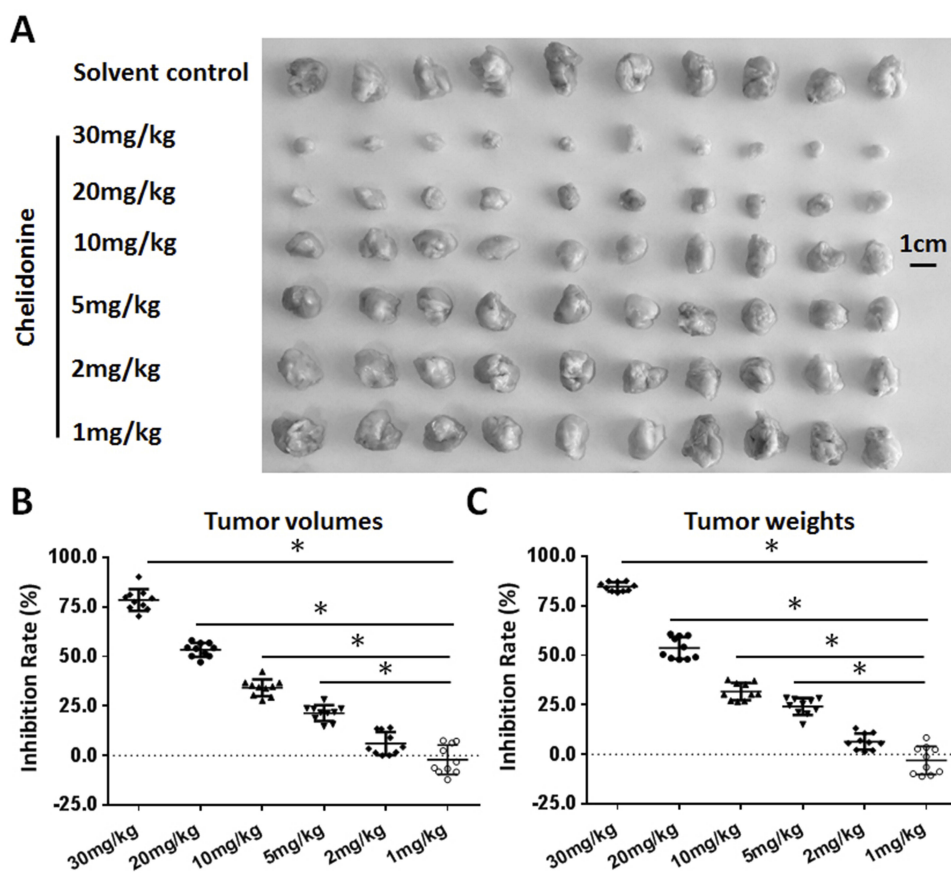


**Figure 3** The antitumor effect of chelidonine on the subcutaneous growth of MHCC97-H cells. MHCC97-H cells were injected into nude mice to form subcutaneous tumor tissues. Mice received the indicated concentrations of chelidonine. The results are shown as photographs (A) or a scatter diagram of inhibition rates calculated from tumor volumes (B) or tumor weights (C). \* $P < 0.05$  versus solvent control with chelidonine.  $n = 10$ .

in Figure 7, MHCC97-H cells form intrahepatic tumor tissues (ie, a lesion) in the liver of nude mice. Treatment of nude mice with 0.5 mg/kg lenvatinib exerts certain antitumor effects on the intrahepatic tumor (Figure 7). Treatment with 5 mg/kg chelidonine alone did not significantly reduce the size of the intrahepatic lesion (Figure 7). However, the combination of lenvatinib with chelidonine significantly enhanced the antitumor effect of lenvatinib (Figure 7). The inhibition rate of lenvatinib on MHCC97-H cells increased from  $34.10 \pm 5.07\%$  to  $52.52 \pm 5.13$ . The expression of EMT-related factors in tumor tissues were shown to confirm the effect of the combination treatment. These data suggested a synergistic effect of chelidonine and lenvatinib in HCC cells.

## Discussion

At present, there is no accurate method for the prediction of the prognosis of advanced HCC patients treated with molecular targeted therapy.<sup>10</sup> Previously, sorafenib was the only molecular targeted therapy option against HCC.<sup>40–43</sup> With

the progress of translational research, new molecular targeted drugs (eg, regorafenib) are gradually becoming clinically applicable. Lenvatinib is a recently approved drug.<sup>44–46</sup> Unfortunately, in HCC patients, a high dose of each agent is required to achieve even limited tumor regression.<sup>47</sup> Therefore, investigation of the detailed mechanisms underlying the resistance to molecular targeted agents, and the development of promising strategies to reduce their effective dosages are warranted.<sup>47</sup> In the present study, we found that treatment with chelidonine enhanced the antitumor effect of lenvatinib on HCC cells. The effect of chelidonine or lenvatinib was also examined in non-tumor L-02 cells. In addition, the effect of the drug was also examined in mice with a normal immune system. Human tumors cannot form tumor tissues in immunologically normal mice. Therefore, tumor tissues were established in immunized normal mice using mouse HCC cells. The results showed that lenvatinib inhibited the formation of subcutaneous tumor by H22 cells. However, the antitumor activity was weaker than that observed in human HCC cells. Chelidonine enhanced the

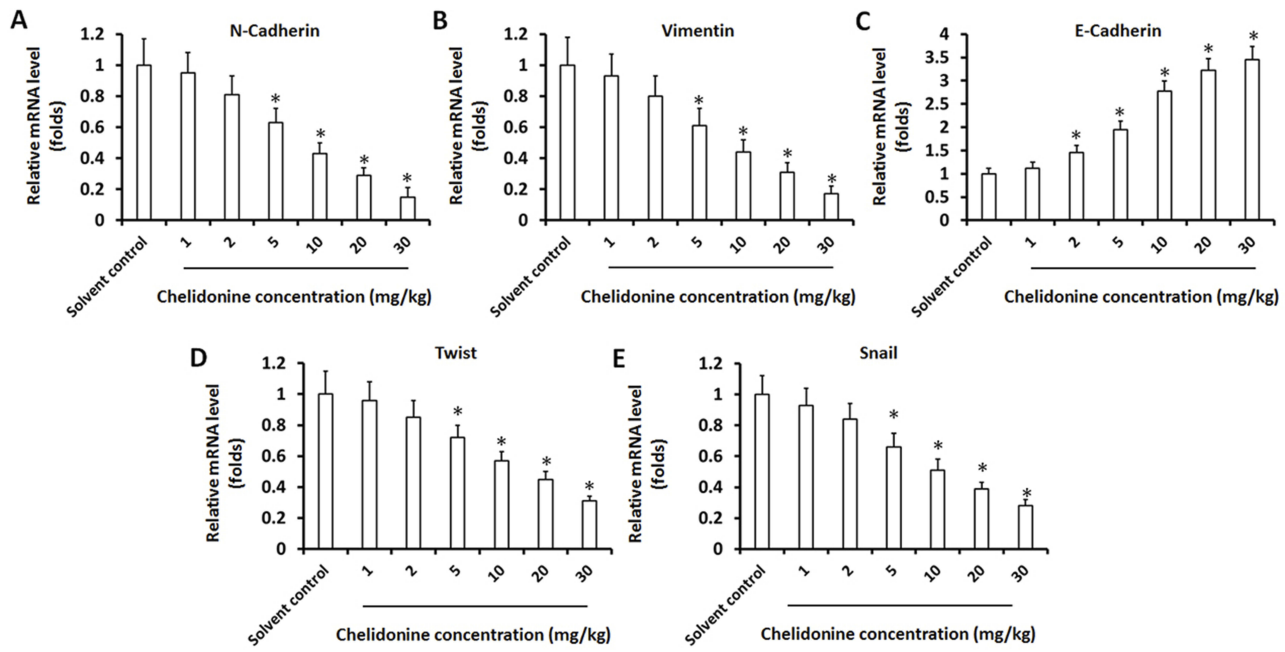


**Figure 4** The effect of chelidonine on EMT indicators or regulators in subcutaneous tumor tissues formed by MHCC97-H cells. MHCC97-H cells were injected into nude mice to form subcutaneous tumor tissues. The mice received the indicated concentrations of chelidonine (1, 2, 5, 10, 20 or 30 mg/kg). Subsequently, the tumor tissues were harvested and the total RNA was extracted from the cells. The expression of N-cadherin (A), Vimentin (B), E-cadherin (C), Twist (D), and Snail (E) was examined through qPCR. The results are shown as the mean  $\pm$  SD from the qPCR experiments.

**Notes:** \* $P < 0.05$  versus solvent control with chelidonine.  $n = 10$ .

**Abbreviations:** EMT, epithelial-mesenchymal transition; qPCR, quantitative polymerase chain reaction; SD, standard deviation.

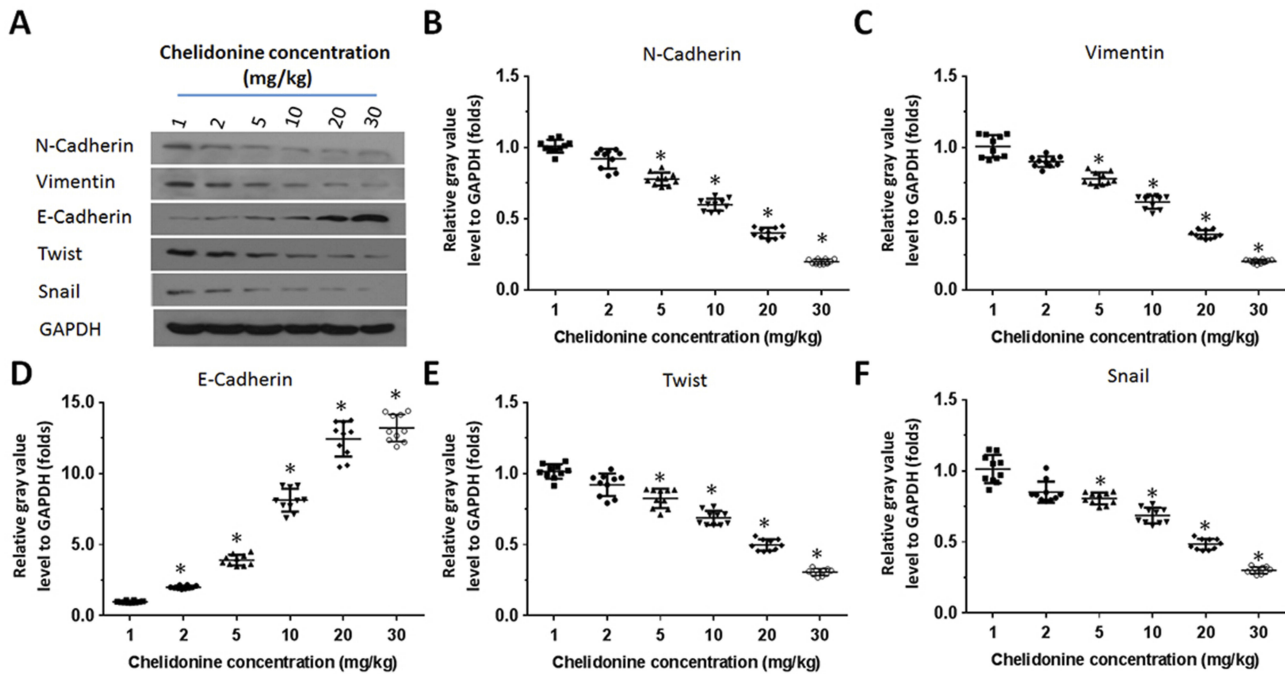


**Figure 5** The effect of chelidonine on EMT indicators or regulators in subcutaneous tumor tissues formed by MHCC97-H cells. MHCC97-H cells were injected into nude mice to form subcutaneous tumor tissues. The mice received the indicated concentrations of chelidonine (1, 2, 5, 10, 20, 30 mg/kg). Subsequently, the tumor tissues were harvested and the total protein was extracted from the cells. The expression of N-cadherin, Vimentin, E-cadherin, Twist, and Snail was examined using Western blotting. GAPDH was selected as a loading control. The results are shown as Western blotting images [A] or a scatter plot of the grayscale scan results (N-cadherin [B], Vimentin [C], E-cadherin [D], Twist [E], and Snail [F]).

**Notes:** \* $P < 0.05$  versus solvent control with chelidonine.  $n = 10$ .

**Abbreviations:** EMT, epithelial-mesenchymal transition; qPCR, quantitative polymerase chain reaction.



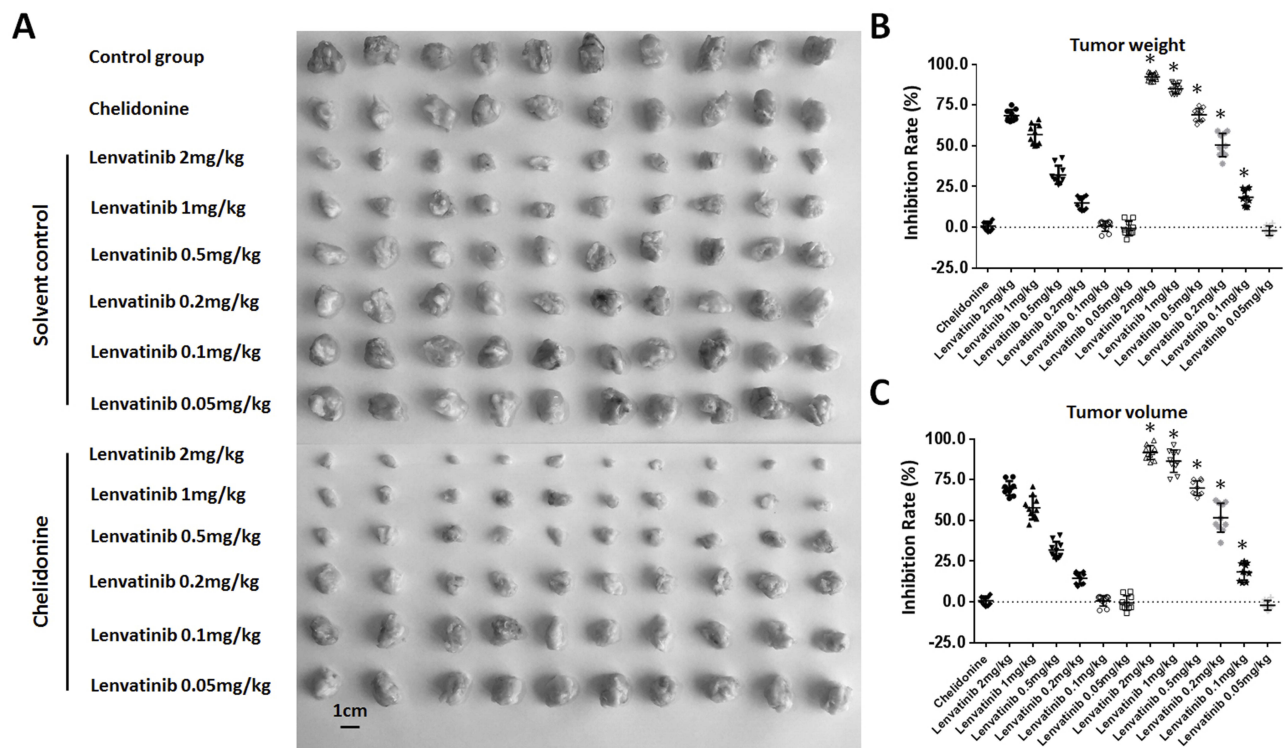


**Figure 6** Chelidonine enhances the antitumor effect of lenvatinib on the subcutaneous growth of MHCC97-H cells. MHCC97-H cells were injected into nude mice to form subcutaneous tumors. Subsequently, the mice received solvent control plus the indicated concentrations of lenvatinib or chelidonine (5 mg/kg) plus the indicated concentrations of lenvatinib. The results are shown as photographs (A) or a scatter diagram of inhibition rates calculated from tumor weights (B) or tumor volumes (C). \* $P < 0.05$  versus solvent control group with chelidonine group.  $n = 10$ .

ability of lenvatinib to inhibit the formation of subcutaneous tumor by H22 cells. This may be attributed to the similarity of various lenvatinib targets (eg, VEGFR or c-Kit) of murine origin to lenvatinib targets (eg, VEGFR or c-Kit) of human origin.

EMT is an important cellular process associated with poor prognosis in HCC patients and mediates metastasis.<sup>48–53</sup> During this process, cell adhesion-related proteins are down-regulated, whereas mesenchymal-related proteins are up-regulated. These effects result in the loss of cell polarity and insensitivity to antitumor drugs.<sup>54,55</sup> It has been shown that EMT is a key factor contributing to the development of resistance to sorafenib.<sup>56–59</sup> Therefore, disruption of the EMT process is a promising strategy to enhance the sensitivity of HCC cells to molecular targeted agents. In the present study, we observed that treatment with chelidonine restricted EMT by modulating its key regulators. Moreover, chelidonine functioned as an antitumor agent through the following mechanisms: (1) Reduction of telomere length; (2) inhibition of the tumor necrosis factor- $\alpha$ /nuclear factor- $\kappa$ B pathways; (3) induction of mitotic slippage and apoptotic-like death; or (4) inhibition of the formation of the integrin-linked kinase/PINCH/ $\alpha$ -

parvin complex.<sup>16,60–66</sup> The findings of the present study extended our knowledge regarding chelidonine and provided useful data for the investigation and development of novel therapeutic strategies against HCC.

Moreover, the biological diversity of the secondary metabolites obtained from natural products provides us with new druggable agents, as well as novel options for chemical synthesis and structural modification.<sup>67–72</sup> Chelidonine could function as an antitumor agent via multi-mechanisms: (1) inducing caspase-dependent or caspase-independent cell death; (2) modulating the telomere length; (3) suppressing the NF- $\kappa$ B pathways; (4) inducing mitotic slippage and apoptotic-like death of human cancer cells.<sup>73–77</sup> In this study, we observed the potential application of chelidonine to the treatment of advanced HCC. We established two in-vivo HCC growth models to examine the in-vivo activity of chelidonine, namely the subcutaneous tumor model and intrahepatic tumor model. MHCC97-H cells were injected into the liver of nude mice to form intrahepatic tumor tissues, mimicking the intrahepatic growth of HCC cells. This model is an accurate tool for HCC-related studies and the evaluation of anti-HCC therapies.

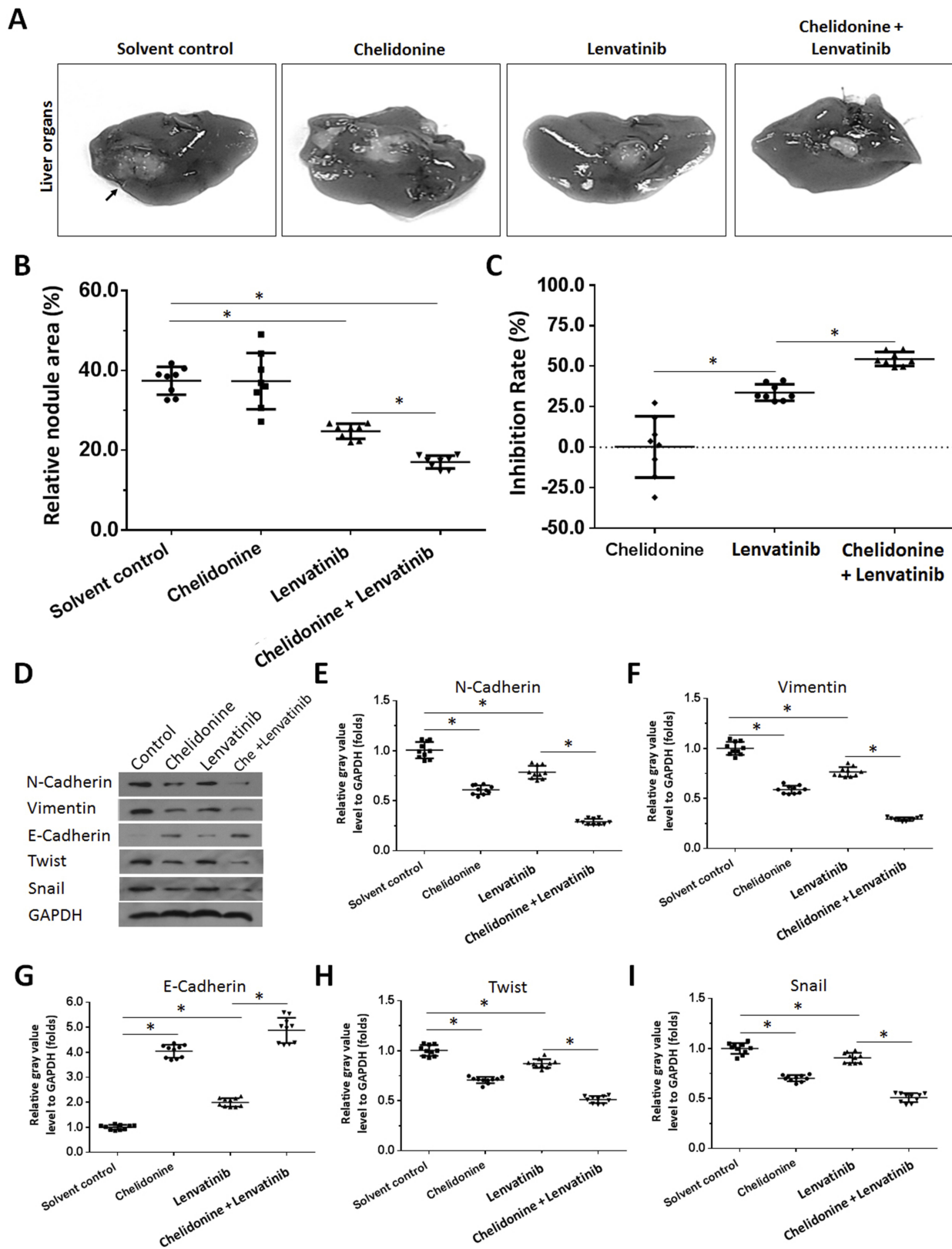


**Figure 7** Chelidone enhances the antitumor effect of lenvatinib on the intrahepatic growth of MHCC97-H cells. MHCC97-H cells were injected into nude mice to form intrahepatic tumors. The mice received solvent control, 5 mg/kg chelidone, 1 mg/kg lenvatinib, or 5 mg/kg chelidone plus 1 mg/kg lenvatinib. The results are shown as photographs of livers with lesions formed by MHCC97-H cells (A), a scatter diagram of lesion/node areas (B), or inhibition rates calculated from the lesion/node areas (C). Subsequently, the tumor tissues were harvested and the total protein was extracted from the cells. The expression of N-cadherin, Vimentin, E-cadherin, Twist, and Snail was examined using Western blotting. GAPDH was selected as a loading control. The results are shown as Western blot images (D) or a scatter plot of the grayscale scan results N-cadherin (E), Vimentin (F), E-cadherin (G), Twist (H), and Snail (I). \* $P < 0.05$  versus solvent control with chelidone.  $n = 10$ .

OncoTargets and Therapy downloaded from <https://www.dovepress.com/> by 146.185.203.32 on 19-Aug-2019  
For personal use only.

## Conclusion

Chelidonine inhibits the process of EMT and enhances the antitumor effect of lenvatinib on HCC cells.

## Abbreviations

HCC, hepatocellular carcinoma; MTT, 3-(4,5-dimethyl-2-thiazolyl)-2,5-diphenyl-2-H- tetrazolium bromide; EMT (epithelial mesenchymal transition); qPCR, quantitative polymerase chain reaction; HBV, hepatitis B virus; VEGFR (vascular endothelial growth factor receptor); MAPK (mitogen-activated protein kinase); DMSO, Dimethyl sulfoxide; DMEM, Dulbecco's Modified Eagle Medium; FBS, fetal bovine serum; IC50 (half maximal inhibitory concentration); qPCR, quantitative polymerase chain reaction; RNA, Ribonucleic Acid; GAPDH, glyceraldehyde-3-phosphate dehydrogenase.

## Acknowledgment

The research was supported financially by the Scientific Research Project of Hebei Administration of Traditional Chinese Medicine, China (Grant No. 2015003), Science and Technology Research Project of Education Department of Hebei province, China (Grant No. BJ2016039, QN2016161), 2017 Traditional Chinese Medicine Resources Survey Project of China (Z135080000022), Natural Science Foundation of Hebei Province of China (Grant No. H2017423048), The National Natural Science Foundation of China (Grant No. 81803762).

## Author contributions

All authors made substantial contributions to the design and conception; acquisition, analysis or interpretation of data. All authors took part in either drafting or revising the manuscript. At the same time, all authors gave final approval of the version to be published; and agree to be accountable for all aspects of the work in ensuring that questions related to the accuracy or integrity of any part of the work are appropriately investigated and resolved.

## Disclosure

The authors report no conflicts of interest in this work.

## References

1. Polaris Observatory Collaborators. Global prevalence, treatment, and prevention of hepatitis B virus infection in 2016: a modelling study. *Lancet Gastroenterol Hepatol*. 2018;3:383–403. doi:10.1016/S2468-1253(18)30056-6
2. Mysore KR, Leung DH. Hepatitis B and C. *Clin Liver Dis*. 2018;22:703–722. doi:10.1016/j.cld.2018.06.002

3. Zhang S, Wang F, Zhang Z. Current advances in the elimination of hepatitis B in China by 2030. *Front Med*. 2017;11:490–501. doi:10.1007/s11684-017-0598-4
4. Wang FS, Fan JG, Zhang Z, Gao B, Wang HY. The global burden of liver disease: the major impact of China. *Hepatology*. 2014;60:2099–2108. doi:10.1002/hep.27406
5. Forner A, Reig M, Bruix J. Hepatocellular carcinoma. *Lancet*. 2018;391:1301–1314. doi:10.1016/S0140-6736(18)30010-2
6. Gailhouse L, Liew LC, Yasukawa K, et al. MEG3-derived miR-493-5p overcomes the oncogenic feature of IGF2-miR-483 loss of imprinting in hepatic cancer cells. *Cell Death Dis*. 2019;10:553. doi:10.1038/s41419-019-1788-6
7. Kudo M, Finn RS, Qin S, et al. Lenvatinib versus sorafenib in first-line treatment of patients with unresectable hepatocellular carcinoma: a randomised phase 3 non-inferiority trial. *Lancet*. 2018;391:1163–1173. doi:10.1016/S0140-6736(18)30207-1
8. Feng F, Jiang Q, Jia H, et al. Which is the best combination of TACE and Sorafenib for advanced hepatocellular carcinoma treatment? A systematic review and network meta-analysis. *Pharmacol Res*. 2018;135:89–101. doi:10.1016/j.phrs.2018.06.021
9. Escudier B, Worden F, Kudo M. Sorafenib: key lessons from over 10 years of experience. *Expert Rev Anticancer Ther*. 2018;1–13. doi:10.1080/14737140.2019.1559058
10. Song Z, Liu T, Chen J, et al. HIF-1 $\alpha$ -induced RIT1 promotes liver cancer growth and metastasis and its deficiency increases sensitivity to sorafenib. *Cancer Lett*. 2019;460:96–107. doi:10.1016/j.canlet.2019.06.016
11. Xie H, Yu H, Tian S, et al. What is the best combination treatment with transarterial chemoembolization of unresectable hepatocellular carcinoma? a systematic review and network meta-analysis. *Oncotarget*. 2017;8:100508–100523. doi:10.18632/oncotarget.20119
12. Bai ZG, Zhang ZT. A systematic review and meta-analysis on the effect of angiogenesis blockade for the treatment of gastric cancer. *Oncotargets Ther*. 2018;11:7077–7087. doi:10.2147/OTT.S169484
13. Mukthinuthalapati VVPK, Wang Y, Abu Omar Y, Syed M, Attar B. Single institution experience of sorafenib for advanced HCC in a US tertiary care hospital. *J Gastrointest Oncol*. 2018;9:833–839. doi:10.21037/jgo.2018.06.09
14. van der Meer AJ, Feld JJ, Hofer H, et al. Risk of cirrhosis-related complications in patients with advanced fibrosis following hepatitis C virus eradication. *J Hepatol*. 2017;66:485–493. doi:10.1016/j.jhep.2016.10.017
15. Liao W, He X, Yi Z, Xiang W, Ding Y. Chelidonine suppresses LPS-Induced production of inflammatory mediators through the inhibitory of the TLR4/NF- $\kappa$ B signaling pathway in RAW264.7 macrophages. *Biomed Pharmacother*. 2018;107:1151–1159. doi:10.1016/j.biopha.2018.08.094
16. Zielińska S, Jezierska-Domaradzka A, Wójciak-Kosior M, Sowa I, Junka A, Matkowski AM. Greater celandine's ups and downs-21 centuries of medicinal uses of chelidonium majus from the viewpoint of today's pharmacology. *Front Pharmacol*. 2018;9:299. doi:10.3389/fphar.2018.00299
17. Noureini SK, Esmaili H, Abachi F, et al. Selectivity of major isoquinoline alkaloids from Chelidonium majus towards telomeric G-quadruplex: A study using a transition-FRET (t-FRET) assay. *Biochim Biophys Acta Gen Subj*. 2017;1861:2020–2030. doi:10.1016/j.bbagen.2017.05.002
18. Havelek R, Seifrtova M, Kralovec K, et al. Comparative cytotoxicity of chelidonine and homochelidonine, the dimethoxy analogues isolated from Chelidonium majus L. (Papaveraceae), against human leukemic and lung carcinoma cells. *Phytomedicine*. 2016;23:253–266. doi:10.1016/j.phymed.2016.01.001
19. Noureini SK, Esmaili H. Multiple mechanisms of cell death induced by chelidonine in MCF-7 breast cancer cell line. *Chem Biol Interact*. 2014;223:141–149. doi:10.1016/j.cbi.2014.09.013

20. El-Readi MZ, Eid S, Ashour ML, Tahrani A, Wink M. Modulation of multidrug resistance in cancer cells by chelidonine and Chelidonium majus alkaloids. *Phytomedicine*. 2013;20(3–4):282–294. doi:10.1016/j.phymed.2012.11.005
21. Chen X, Yu J, Zhong B, et al. Pharmacological activities of dihydrotanshinone I, a natural product from *Salvia miltiorrhiza* Bunge. *Pharmacol Res*. 2019;145:104254. doi:10.1016/j.phrs.2019.104254
22. Xiang X, Cai HD, Su SL, et al. *Salvia miltiorrhiza* protects against diabetic nephropathy through metabolome regulation and wnt/ $\beta$ -catenin and TGF- $\beta$  signaling inhibition. *Pharmacol Res*. 2019;139:26–40. doi:10.1016/j.phrs.2018.10.030
23. Choy KW, Murugan D, Mustafa MR. Natural products targeting ER stress pathway for the treatment of cardiovascular diseases. *Pharmacol Res*. 2018;132:119–129. doi:10.1016/j.phrs.2018.04.013
24. Jia H, Yang Q, Wang T, et al. Rhamnetin induces sensitization of hepatocellular carcinoma cells to a small molecular kinase inhibitor or chemotherapeutic agents. *Biochim Biophys Acta*. 2016;1860:1417–1430. doi:10.1016/j.bbagen.2016.04.007
25. Shao Z, Li Y, Dai W, et al. ETS-1 induces Sorafenib-resistance in hepatocellular carcinoma cells via regulating transcription factor activity of PXR. *Pharmacol Res*. 2018;135:188–200. doi:10.1016/j.phrs.2018.08.003
26. Feng F, Jiang Q, Cao S, et al. Pregnane X receptor mediates sorafenib resistance in advanced hepatocellular carcinoma. *Biochim Biophys Acta Gen Subj*. 2018;1862:1017–1030. doi:10.1016/j.bbagen.2018.01.011
27. Feng F, Lu YY, Zhang F, et al. Long interspersed nuclear element ORF-1 protein promotes proliferation and resistance to chemotherapy in hepatocellular carcinoma. *World J Gastroenterol*. 2013;19:1068–1078. doi:10.3748/wjg.v19.i7.1068
28. Li F, Wei A, Bu L, et al. Pro-caspase-3-activating compound 1 stabilizes hypoxia-inducible factor 1 $\alpha$  and induces DNA damage by sequestering ferrous iron. *Cell Death Dis*. 2018;9:1025. doi:10.1038/s41419-018-1038-3
29. Guan F, Ding R, Zhang Q, et al. WX-132-18B, a novel microtubule inhibitor, exhibits promising anti-tumor effects. *Oncotarget*. 2017;8:71782–71796. doi:10.18632/oncotarget.17710
30. Ji Q, Xu X, Li L, et al. miR-216a inhibits osteosarcoma cell proliferation, invasion and metastasis by targeting CDK14. *Cell Death Dis*. 2017;8:e3103. doi:10.1038/cddis.2017.499
31. Liang Y, Xu X, Wang T, et al. The EGFR/miR-338-3p/EYA2 axis controls breast tumor growth and lung metastasis. *Cell Death Dis*. 2017;8:e2928. doi:10.1038/cddis.2017.325
32. Li J, Zhao J, Wang H, et al. MicroRNA-140-3p enhances the sensitivity of hepatocellular carcinoma cells to sorafenib by targeting pregnenolone X receptor. *Onco Targets Ther*. 2018;11:5885–5894. doi:10.2147/OTT.S179509
33. Zhang Y, Li D, Jiang Q, et al. Novel ADAM-17 inhibitor ZLDI-8 enhances the in vitro and in vivo chemotherapeutic effects of Sorafenib on hepatocellular carcinoma cells. *Cell Death Dis*. 2018;9:743. doi:10.1038/s41419-018-0804-6
34. Xie H, Tian S, Yu H, et al. A new apatinib microcrystal formulation enhances the effect of radiofrequency ablation treatment on hepatocellular carcinoma. *Onco Targets Ther*. 2018;11:3257–3265. doi:10.2147/OTT.S165000
35. Li L, Liang Y, Kang L, et al. Transcriptional regulation of the warburg effect in cancer by SIX1. *Cancer Cell*. 2018;33:368–385. doi:10.1016/j.ccell.2018.01.010
36. Meng D, Lei M, Han Y, et al. MicroRNA-645 targets urokinase plasminogen activator and decreases the invasive growth of MDA-MB-231 triple-negative breast cancer cells. *Onco Targets Ther*. 2018;11:7733–7743. doi:10.2147/OTT.S187221
37. Meng D, Meng M, Luo A, et al. Effects of VEGFR1+ hematopoietic progenitor cells on pre-metastatic niche formation and in vivo metastasis of breast cancer cells. *J Cancer Res Clin Oncol*. 2019;145:411–427. doi:10.1007/s00432-018-2802-6
38. Meng D, Lei H, Zheng X, et al. A temperature-sensitive phase-change hydrogel of tamoxifen achieves the long-acting antitumor activation on breast cancer cells. *Onco Targets Ther*. 2019;12:3919–3931. doi:10.2147/OTT.S201421
39. Chen Y, Zeng Q, Liu X, et al. LINE-1 ORF-1p enhances the transcription factor activity of pregnenolone X receptor and promotes sorafenib resistance in hepatocellular carcinoma cells. *Cancer Manag Res*. 2018;10:4421–4438. doi:10.2147/CMAR.S176088
40. Roskoski R Jr. Properties of FDA-approved small molecule protein kinase inhibitors. *Pharmacol Res*. 2019;144:19–50. doi:10.1016/j.phrs.2019.03.006
41. Lacial PM, Graziani G. Therapeutic implication of vascular endothelial growth factor receptor-1 (VEGFR-1) targeting in cancer cells and tumor microenvironment by competitive and non-competitive inhibitors. *Pharmacol Res*. 2018;136:97–107. doi:10.1016/j.phrs.2018.08.023
42. Roskoski R Jr. Targeting oncogenic Raf protein-serine/threonine kinases in human cancers. *Pharmacol Res*. 2018;135:239–258. doi:10.1016/j.phrs.2018.08.013
43. Roskoski R Jr. The role of small molecule platelet-derived growth factor receptor (PDGFR) inhibitors in the treatment of neoplastic disorders. *Pharmacol Res*. 2018;129:65–83. doi:10.1016/j.phrs.2018.01.021
44. Reig M, Bruix J. Lenvatinib: can a non-inferiority trial change clinical practice? *Lancet*. 2018;391:1123–1124. doi:10.1016/S0140-6736(18)30208-3
45. Pavlakis N, Sjoquist KM, Martin AJ, et al. Regorafenib for the treatment of advanced gastric cancer (INTEGRATE): a multinational placebo-controlled Phase II trial. *J Clin Oncol*. 2016;34:2728–2735. doi:10.1200/JCO.2015.65.1901
46. Bruix J, Qin S, Merle P, et al.; RESORCE Investigators. Regorafenib for patients with hepatocellular carcinoma who progressed on sorafenib treatment (RESORCE): a randomised, double-blind, placebo-controlled, phase 3 trial. *Lancet*. 2017;389:56–66. doi:10.1016/S0140-6736(16)32453-9
47. Zhu YJ, Zheng B, Wang HY, Chen L. New knowledge of the mechanisms of sorafenib resistance in liver cancer. *Acta Pharmacol Sin*. 2017;38:614–622. doi:10.1038/aps.2017.5
48. Wang XM, Li QY, Ren LL, et al. Effects of MCRS1 on proliferation, migration, invasion, and epithelial mesenchymal transition of gastric cancer cells by interacting with Pkmyt1 protein kinase. *Cell Signal*. 2019;59:171–181. doi:10.1016/j.cellsig.2019.04.002
49. Zou Y, Li S, Li Z, Song D, Zhang S, Yao Q. MiR-146a attenuates liver fibrosis by inhibiting transforming growth factor- $\beta$ 1 mediated epithelial-mesenchymal transition in hepatocytes. *Cell Signal*. 2019;58:1–8. doi:10.1016/j.cellsig.2019.01.012
50. Kim SH, Lee WH, Kim SW, et al. EphA3 maintains radioresistance in head and neck cancers through epithelial mesenchymal transition. *Cell Signal*. 2018;47:122–130. doi:10.1016/j.cellsig.2018.04.001
51. Liu GM, Li Q, Zhang PF, et al. Restoration of FBP1 suppressed Snail-induced epithelial to mesenchymal transition in hepatocellular carcinoma. *Cell Death Dis*. 2018;9:1132. doi:10.1038/s41419-018-1165-x
52. Wu X, Zhao J, Ruan Y, Sun L, Xu C, Jiang H. Sialyltransferase ST3GAL1 promotes cell migration, invasion, and TGF- $\beta$ 1-induced EMT and confers paclitaxel resistance in ovarian cancer. *Cell Death Dis*. 2018;9:1102. doi:10.1038/s41419-018-1101-0
53. Sun J, Xu Z, Lv H, et al. eIF5A2 regulates the resistance of gastric cancer cells to cisplatin via induction of EMT. *Am J Transl Res*. 2018;10:4269–4279.
54. Takagi K, Yamakuchi M, Matsuyama T, et al. IL-13 enhances mesenchymal transition of pulmonary artery endothelial cells via down-regulation of miR-424/503 in vitro. *Cell Signal*. 2018;42:270–280. doi:10.1016/j.cellsig.2017.10.019
55. Chatterjee S, Sil PC. Targeting the crosstalks of Wnt pathway with Hedgehog and Notch for cancer therapy. *Pharmacol Res*. 2019;142:251–261. doi:10.1016/j.phrs.2019.02.027



56. Gunes A, Bagirsakci E, Iscan E, et al. Thioredoxin interacting protein promotes invasion in hepatocellular carcinoma. *Oncotarget*. 2018;9:36849–36866. doi:10.18632/oncotarget.26402
57. Tripathi V, Shin JH, Stuelten CH, Zhang YE. TGF- $\beta$ -induced alternative splicing of TAK1 promotes EMT and drug resistance. *Oncogene*. 2019;38:3185–3200. doi:10.1038/s41388-018-0655-8
58. Tan W, Luo X, Li W, et al. TNF- $\alpha$  is a potential therapeutic target to overcome sorafenib resistance in hepatocellular carcinoma. *EBioMedicine*. 2019;40:446–456. doi:10.1016/j.ebiom.2018.12.047
59. Zhang PF, Wang F, Wu J, et al. LncRNA SNHG3 induces EMT and sorafenib resistance by modulating the miR-128/CD151 pathway in hepatocellular carcinoma. *J Cell Physiol*. 2019;234:2788–2794. doi:10.1002/jcp.27095
60. Qin CD, Ma DN, Zhang SZ, et al. The Rho GTPase Rnd1 inhibits epithelial-mesenchymal transition in hepatocellular carcinoma and is a favorable anti-metastasis target. *Cell Death Dis*. 2018;9:486. doi:10.1038/s41419-018-0517-x
61. Chung CL, Wang SW, Sun WC, et al. Sorafenib suppresses TGF- $\beta$  responses by inducing caveolae/lipid raft-mediated internalization/degradation of cell-surface type II TGF- $\beta$  receptors: Implications in development of effective adjunctive therapy for hepatocellular carcinoma. *Biochem Pharmacol*. 2018;154:39–53. doi:10.1016/j.bcp.2018.04.014
62. Liu Y, Peng Y, Zhang Z, Guo X, Ji M, Zheng J. In vitro and in vivo studies of the metabolic activation of chelidonine. *Chem Biol Interact*. 2019;308:155–163. doi:10.1016/j.cbi.2019.05.012
63. Herrmann R, Roller J, Polednik C, Schmidt M. Effect of chelidonine on growth, invasion, angiogenesis and gene expression in head and neck cancer cell lines. *Oncol Lett*. 2018;16:3108–3116. doi:10.3892/ol.2018.9031
64. Qing ZX, Huang JL, Yang XY, et al. Anticancer and reversing multi-drug resistance activities of natural isoquinoline alkaloids and their structure-activity relationship. *Curr Med Chem*. 2018;25:5088–5114. doi:10.2174/0929867324666170920125135
65. Wang X, Tanaka M, Krstin S, Peixoto HS, Wink M. The interference of selected cytotoxic alkaloids with the cytoskeleton: an insight into their modes of action. *Molecules*. 2016;21:pii: E906. doi:10.3390/molecules21070906
66. Kim O, Hwangbo C, Kim J, Li DH, Min BS, Lee JH. Chelidonine suppresses migration and invasion of MDA-MB-231 cells by inhibiting formation of the integrin-linked kinase/PINCH/ $\alpha$ -parvin complex. *Mol Med Rep*. 2015;12:2161–2168. doi:10.3892/mmr.2015.3621
67. Koriem KM, Arbid MS, Asaad GF. Chelidonium majus leaves methanol extract and its chelidonine alkaloid ingredient reduce cadmium-induced nephrotoxicity in rats. *J Nat Med*. 2013;67:159–167. doi:10.1007/s11418-012-0667-6
68. Noureini SK, Wink M. Transcriptional down regulation of hTERT and senescence induction in HepG2 cells by chelidonine. *World J Gastroenterol*. 2009;15(29):3603–3610. doi:10.3748/wjg.15.3603
69. Zheng G, Shen Z, Chen H, et al. Metapristone suppresses non-small cell lung cancer proliferation and metastasis via modulating RAS/RAF/MEK/MAPK signaling pathway. *Biomed Pharmacother*. 2017;90:437–445. doi:10.1016/j.biopha.2017.03.091
70. Fan Y, Lu H, An L, et al. Effect of active fraction of Eriocaulon sieboldianum on human leukemia K562 cells via proliferation inhibition, cell cycle arrest and apoptosis induction. *Environ Toxicol Pharmacol*. 2016;43:13–20. doi:10.1016/j.etap.2015.11.001
71. Fan Y, Lu H, Ma H, et al. Bioactive compounds of Eriocaulon sieboldianum blocking proliferation and inducing apoptosis of HepG2 cells might be involved in Aurora kinase inhibition. *Food Funct*. 2015;6:3746–3759. doi:10.1039/c5fo00371g
72. Awortwe C, Bruckmueller H, Cascorbi I. Interaction of herbal products with prescribed medications: A systematic review and meta-analysis. *Pharmacol Res*. 2019;141:397–408. doi:10.1016/j.phrs.2019.01.028
73. Lee YK, Lee KW, Kim M, et al. Chelidonine induces caspase-dependent and caspase-independent cell death through G2/M arrest in the T98G human glioblastoma cell line. *Evid Based Complement Alternat Med*. 2019;2019:6318179. doi:10.1155/2019/6318179
74. Kazemi Noureini S, Fatemi L, Wink M. Telomere shortening in breast cancer cells (MCF7) under treatment with low doses of the benzylisoquinoline alkaloid chelidonine. *PLoS One*. 2018;13:e0204901. doi:10.1371/journal.pone.0204901
75. Wang X, Decker CC, Zechner L, Krstin S, Wink M. In vitro wound healing of tumor cells: inhibition of cell migration by selected cytotoxic alkaloids. *BMC Pharmacol Toxicol*. 2019;20:4. doi:10.1186/s40360-018-0284-4
76. Zhang ZH, Mi C, Wang KS, et al. Chelidonine inhibits TNF- $\alpha$ -induced inflammation by suppressing the NF- $\kappa$ B pathways in HCT116 cells. *Phytother Res*. 2018;32:65–75. doi:10.1002/ptr.5948
77. Qu Z, Zou X, Zhang X, et al. Chelidonine induces mitotic slippage and apoptotic-like death in SGC-7901 human gastric carcinoma cells. *Mol Med Rep*. 2016;13:1336–1344. doi:10.3892/mmr.2015.4683

## OncoTargets and Therapy

### Publish your work in this journal

OncoTargets and Therapy is an international, peer-reviewed, open access journal focusing on the pathological basis of all cancers, potential targets for therapy and treatment protocols employed to improve the management of cancer patients. The journal also focuses on the impact of management programs and new therapeutic

agents and protocols on patient perspectives such as quality of life, adherence and satisfaction. The manuscript management system is completely online and includes a very quick and fair peer-review system, which is all easy to use. Visit <http://www.dovepress.com/testimonials.php> to read real quotes from published authors.

Submit your manuscript here: <https://www.dovepress.com/oncotargets-and-therapy-journal>

Dovepress